Palestine Journal of Mathematics

Vol. 11(Special Issue I)(2022) , 75–85

ROBUST SURFACE RECONSTRUCTION IN FOURIER DOMAIN USING MATHEMATICAL MORPHOLOGY

Anu Bala

Communicated by Shimpi Singh Jadon

MSC 2010 Classifications: 42B10, 97R20, 65K05, 97N60.

Keywords and phrases: Discrete Fourier Transform, Image segmentation, Morphological operations, Noisy images, Surface gradients, Surface Reconstruction.

Abstract In this study, an efficient and robust algorithm is proposed for surface reconstruction from a noisy image. In the noisy image, degraded gradient field is obtained and used as input. The proposed approach is based upon the image segmentation using some basic morphological operations. Afterwards, sort out the position of the pixels of unit intensity from the segmented image. Then take the intensity values of those particular pixels from the given image. Thus sparse data of intensity values from the image is used rather than whole intensity values of the image. This helps to guarantee good surface reconstruction in case of noisy images. The surface fitting is done using the cubic spline method. The surface obtained in crude form, is further refined using the error minimization of the gradients. The performance of the proposed method is exhibited using synthetic and real data. Experimental results demonstrate that our methodology produces accurate surface reconstruction that preserves remarkable and sharp features.

1 Introduction

Loads of shape attaining algorithms for instance shape from shading [10], shape from texture [19] and photometric stereo [26] merely generate the surface normals of a real object. Some integration process needs to be followed to infer the surface shape from these normals. Nevertheless, the reconstruction by the use of the integration process is sensitive to the noise as well as to the selection of integration path across the surface. The authors in [23] has provided denoising with edge preservation in noisy digital images. Integration is also considered as a mathematical tool to redeem an image using incomplete Fourier parameters after finding the image gradients by the use of Compressed Sensing techniques [17]. In [20], derivative compressed sensing technique (DCS) technique, a modification of compressed sensing is used to reconstruct the surface from the gradient field. This shape recovery of the three-dimensional (3D) surface from the two-dimensional (2D) images has an ample variety of applications viz. 3D reconstruction (surgery, remote sensing, architecture), the distance calculation (vehicle control, robotics), reconstruction of planet surfaces from their images captured by aircraft and satellites.

The most basic approach to reconstruct a surface from its corresponding gradients depends on the minimization of the cost function using least square technique. This results in the generation of Poisson's equation which can be solved by various methods [21]. However this approach has been plagued by some problems arising in case of noisy images. Alternatively, decomposition of images into basis functions is widely popular among researchers. The researchers have accomplished this analysis by the correlation of the considered basis functions and image intensity or pixel values to generate a vector of coefficients. Then the reconstruction has been performed by combining these basis functions linearly. Frankot and Chellapa [7] proposed Fourier basis functions, while Kovesi [12] performed the reconstruction of surfaces using shapelets as a non-orthogonal set of basis functions. An algorithm has been proposed in [25] based upon Fourier transform method to get the height from the gradients. Some modified algorithms have been described in [24] for the process of image inpainting in Fourier transform domain. In [5], surface reconstruction was performed by solving the Poisson's equation using discrete Fourier sine transform. The methods in [8] used spectral, Tikhonov and constrained regularization to get better least squares fit. Some authors also used regularizations in reconstructing the surface using its corresponding gradients in the photometric stereo for the industrial applications [9]. This approach can reconstruct the mega-pixel sized surface in a few seconds.

Agrawal et al. [2] proposed a generalized structure for the extension of the Poisson equation. The authors in [1] proposed an another method to correct the gradient field with some algebraic method. The outcomes of the proposed method are impressive when the corresponding gradient field is disturbed with the outliers only, but unhappily, the results are less acceptable in the occurrence of noise. In [11], a noise reduction technique is proposed for surface reconstruction from noisy gradient fields. The methods discussed so far, perform well either in the presence of noise only or the outliers only, but not in the case, when both outliers and noise are assorted. But in general, most of the real world data usually contains the mixture of noise as well as outliers. The literature reveals that the methods based on l_1-minimization can handle the outliers in a better way. The method proposed in [18] handled the problem as a residual gradient error correction by taking into account the l_1-norm. l_1-based methods can handle three cases, outliers only, noise only, both noise and outliers. Nevertheless, these methods are not able to reconstruct a high quality surface in case of rigorously corrupted gradient field.

While most methods to obtain the surface from the gradient field return discrete height values as an output, few methods are efficient to reconstruct a continuous surface. The method proposed in [15], reconstructed a 3D continuous surface from a gradient field without imposing the discrete integrability constraint. Their method incorporated Gaussian kernel basis functions to reconstruct the continuous surface into high dimensional space. In [13], feed-forward neural network was employed to improve the depth values on the basis of scale invariant features (SIFT) indexes. An algorithm for reconstructing a digital object based upon morphing approach was given in [14], which helps in kidney animation and tumour tracking. In [28], an another technique to reconstruct textured mesh surfaces was presented where point cloud is rendered by patch-based multi view stereo approach. In [4], a new optimization approach was presented for reconstruction of the surface based upon triple sparsity prior with an ability to handle both outliers and noise. In [22], a method for 3D shape measurement was proposed using a camera and a periscope. In [6], an algorithm for 3D depth estimation was presented by the use of wavelet transform. The authors concluded that their approach produced a very efficient depth perception model with minimal hardware involvement. In [27], 3D objects are constructed from minimum number of images, using Wide Baseline Matching and 3D registration algorithm.

This study presents a new approach to reconstruct the surface from sparse data of image intensities. This operation of getting sparse data is performed by image segmentation using morphological operations. Firstly intensities are evaluated only at few pixels in the segmented image and then surface fitting is performed using the cubic spline method to get intermediate surface in crude form. Afterwards, gradient field is estimated from this intermediate surface and again the height in refined form is recovered from the error minimization of the gradient field. Thus use of sparse intensity data initially, results in an accurate surface reconstruction from noisy images. The proposed approach differs from recently depth acquisition sensors. For example, it works in all scenario while kinect works only in indoor environment.

The organization of different sections in this paper is specified as following: a concise overview of the proposed algorithm for surface reconstruction is given in the Section 2. Section 3 explores the experimental results and finally paper is concluded in Section 4.

2 Surface Reconstruction

The process of 3D surface reconstruction from a noisy image is divided into following three phases:

- **Phase 1**: Segmentation of the image using the mathematical morphological operations.
- **Phase 2**: Intermediate surface fitting using cubic spline interpolation.
- **Phase 3**: Recovering depth map by calculating the gradients from the intermediate surface using minimization of error flanked by the evaluated gradients and the gradients of the surface to be recovered.

Before going through these three phases, firstly the input noisy image is preprocessed by performing the convolution process on it with a Gaussian filter of appropriate variance.

2.1 Segmentation Using Mathematical Morphology

Mathematical morphology is a technique to extract geometric information from the intensity values of the images. A shape probe identified as structuring element (SE) is used to extract this type of information. The nature of the output information relies on the shape and size of SE. Image segmentation is a grouping process that enables image pixels to be separated on the basis of their intensity values. One of the segmentation schemes is hard thresholding or binarisation, where a threshold is decided manually or experimentally. However, this type of segmentation may lead to false grouping outcomes, if the image pixels are crowded. To avoid this type of erroneous segmentation, we take the help of mathematical morphology operations using some appropriate structuring elements. In practice, the shape and size of the SE must be fitted to the image that has to be processed. The primary morphological operations are dilation and erosion, since all other operations are based on their combinations. In our proposed algorithm, one of the most important operations, is the blend of dilation and erosion, called opening has been employed.

The process of erosion followed by dilation is called the opening. Let A be an intensity image and B as a structuring element, the opening of A by B, denoted by $A \circ B$ is defined as:

$$A \circ B = (A \Theta B) \oplus B$$

Geometrically, opening is the union of all translations of B that adapt completely within A. Morphological opening removes regions of an image entirely that cannot contain the SE, generally smooths the boundaries of larger objects without changing their area, and eliminates small and thin protrusions. Morphological openings are always anti-extensive transformations, i.e. some pixels are removed. Once the opening process of the image is over, then this opened image is subtracted from the original one called a top-hat transformation, denoted by $TH_B(A)$.

$$TH_B(A) = A - (A \circ B)$$

Where, A is the original input image and B is the structuring element. The main advantage of top-hat approach is to recover those image structures which have removed by the SE during the opening process. After implementing top-hat transformation, the gray level image is converted to binary image using binary thresholding transformation. Thresholds are categorized as global or local, i.e. they remain constant throughout the image, or vary spatially. In our approach, we choose global optimal threshold using a method proposed by Otsu [16].

2.2 Intermediate Surface Fitting

In the next step, only those pixels from the segmented binary image are considered, where the intensity value is unity. The corresponding positioned pixels from the input noisy image are further used for intermediate surface fitting. Thus we use sparse data of noisy image for surface reconstruction rather than the whole image pixels. The intensity values on these pixels are taken into account for further step of surface fitting. Surface fitting is done using the cubic spline interpolation. A cubic polynomial is fitted between the sets of three data points of the surfaces using cubic spline interpolation. The cubic spline has second order continuity at the joints. The cubic spline is characterized over a rectangle R in the plane (x, y), whose sides are parallel to x-axis as well as y-axis. This rectangle R is split into rectangular panels using the lines, which are parallel to x-axis and y-axis. This cubic spline is a cubic polynomial over each panel,. Mathematically, the expression for a single cubic spline segment over each spline is given by:

$$\sum_{i=0}^{3} \sum_{j=0}^{3} a_{ij} x^i y^j$$

Every cubic polynomial in each rectangular panel connects the spline in adjoining panels with a continuity upto second order derivative. The set of interior knots for the variable x of a cubic spline is formed by the constant x-values of the separating lines, parallel to the y-axis. Similarly, for the variable y of the cubic spline, the set of interior knots is formed by the constant y-values of separating lines, parallel to the x-axis.

2.3 Recovering depth map from gradients of intermediate surface

In this section, refined depth map is recovered from intermediate surface gradients, which, in turn, utilized for reconstruction of surface. Let $\nabla Z_{int} = (p, q)$ denotes the given gradient field evaluated on the intermediate surface $Z_{int}(x, y)$ points. These gradients are computed by utilizing central difference operator inside the grid of the discretized surface and by utilizing suitable forward and backward difference operator over the edges of the grid. The surface gradients (p, q) are computed by using the formulae as given below:

$$p_{\imath,\jmath} = \begin{cases} \frac{Z_{int}(\imath+1,\jmath)-Z_{int}(\imath-1,\jmath)}{2} & \forall \quad (\imath,\jmath) \in \text{grid interior} \\ Z_{int}(\imath+1,\jmath) - Z_{int}(\imath,\jmath) & \forall \quad (\imath,\jmath) \in \text{left edge} \\ Z_{int}(\imath,\jmath) - Z_{int}(\imath-1,\jmath) & \forall \quad (\imath,\jmath) \in \text{right edge} \end{cases}$$

$$q_{\imath,\jmath} = \begin{cases} \frac{Z_{int}(\imath,\jmath+1)-Z_{int}(\imath,\jmath-1)}{2} & \forall \quad (\imath,\jmath) \in \text{grid interior} \\ Z_{int}(\imath,\jmath+1) - Z_{int}(\imath,\jmath) & \forall \quad (\imath,\jmath) \in \text{upper edge} \\ Z_{int}(\imath,\jmath) - Z_{int}(\imath,\jmath-1) & \forall \quad (\imath,\jmath) \in \text{lower edge} \end{cases}$$

Let $U(x, y)$ be the required discrete depth map to recover and $\nabla U = (U_x, U_y)$ be the true gradient of U. The objective is to calculate a depth map $U(x, y)$ in the way, such as

$$U_x = \frac{\partial U}{\partial x} = p, \quad U_y = \frac{\partial U}{\partial y} = q$$

The optimal value of depth map $U(x, y)$ may be evaluated by minimizing the following error function in the image domain Ω as:

$$J(U) = \iint_{\Omega} \left[(U_x - p)^2 + (U_y - q)^2\right] dxdy \tag{2.1}$$

Suppose that the required depth map U may be described as a linear sum of basis functions $\psi(x, y; \Omega)$, here $\Omega = (u, v)$.

$$U(x, y) = \sum_{\Omega} C(\Omega)\psi(x, y; \Omega) \tag{2.2}$$

Differentiate equation (2.2) w.r.t. x and y, and we get:

$$\frac{\partial U}{\partial x} = \sum_{w} C(\Omega)\psi_x(x, y; \Omega) \tag{2.3}$$

$$\frac{\partial U}{\partial y} = \sum_{\Omega} C(\Omega)\psi_y(x, y; \Omega) \tag{2.4}$$

Now, $p(x, y)$ and $q(x, y)$ are defined as:

$$p = \sum_{\Omega} C_1(\Omega)\psi_x(x, y; \Omega) \tag{2.5}$$

$$q = \sum_{\Omega} C_2(\Omega)\psi_y(x, y; \Omega) \tag{2.6}$$

To assess the estimation of the coefficients $C(\Omega)$ defined in the equation (2.2), two new parameters K_1 and K_2 are presented as:

$$K_1(\Omega) = \iint |\psi_x(x, y; \Omega)|^2 dxdy \tag{2.7}$$

$$K_2(\Omega) = \iint |\psi_y(x, y; \Omega)|^2 dxdy \tag{2.8}$$

The optimal estimation of the coefficients $C(\Omega)$ defined in equation (2.2), which in turn, used to minimize the error function provided in equation (2.1) is computed as;

$$C(\Omega) = \frac{K_1(\Omega)C_1(\Omega) + K_2(\Omega)C_2(\Omega)}{K_1(\Omega) + K_2(\Omega)} \tag{2.9}$$

In the proposed approach, discrete Fourier basis has been employed in support of its computational efficiency. Here,

$$\psi(x,y;\Omega) = exp\left(2\pi i\left(\frac{xu}{M}+\frac{yv}{N}\right)\right) \tag{2.10}$$

After differentiating the Fourier basis w.r.t. x and y, we obtain:

$$\begin{aligned}\psi_x &= \left(2\pi i\frac{u}{M}\right)\psi(x,y;\Omega)\\ \psi_y &= \left(2\pi i\frac{v}{N}\right)\psi(x,y;\Omega)\end{aligned} \tag{2.11}$$

The coefficients K_1 and K_2 may be evaluated by utilizing equation (2.7) as follows:

$$K_1(\Omega) = \left(\frac{2\pi u}{M}\right)^2; \qquad K_2(\Omega) = \left(\frac{2\pi v}{N}\right)^2 \tag{2.12}$$

From the (2.5) and (2.6), by taking the Discrete Fourier Transform (DFT) of p and q, composed as $\mathcal{F}(p)$ and $\mathcal{F}(q)$, the expansion coefficients $C_1(\Omega)$ and $C_2(\Omega)$ are determined as:

$$C_1(\Omega) = \frac{-iMN}{2\pi u}\frac{\mathcal{F}(p)}{N}; \quad C_2(\Omega) = \frac{-iMN}{2\pi v}\frac{\mathcal{F}(q)}{M} \tag{2.13}$$

Now, to get $C(\Omega)$, substitute the values of C_1, C_2, K_1 and K_2 from equation (2.12) and (2.13) in equation (2.9). On substituting this value of $C(\Omega)$ in equation (2.2) and afterwards by taking the DFT of equation (2.2), we obtain:

$$\begin{aligned}\mathcal{F}(U) &= -i\left(\frac{\frac{2\pi u}{M}\mathcal{F}(p)+\frac{2\pi v}{N}\mathcal{F}(q)}{(\frac{2\pi u}{M})^2+(\frac{2\pi v}{N})^2}\right)\\ &= \frac{-i}{2\pi}\left(\frac{\frac{u}{M}\mathcal{F}(p)+\frac{v}{N}\mathcal{F}(q)}{(\frac{u}{M})^2+(\frac{v}{N})^2}\right)\end{aligned} \tag{2.14}$$

Now, the final output U w.r.t. input p and q may be composed as:

$$U = \mathcal{F}^{-1}\left(\frac{-i}{2\pi}\left(\frac{\frac{u}{M}\mathcal{F}(p)+\frac{v}{N}\mathcal{F}(q)}{(\frac{u}{M})^2+(\frac{v}{N})^2}\right)\right) \tag{2.15}$$

Here $\mathcal{F}(\cdot)$ and $\mathcal{F}^{-1}(\cdot)$ denote Discrete Fourier Transform (DFT) and inverse Discrete Fourier Transform (IDFT) operations respectively. Using equation (2.15), the depth map (height data) $U(x,y)$ has been determined at discrete points, which in turn, employed in reconstructing 3D surface. The whole performed task has been illustrated in a block diagram shown in Fig. 1.

3 Results and Discussions

Our proposed algorithm has been implemented on various real as well as synthetic noisy images to recover depth information from these images and then reconstruct 3D surface in a very efficient manner. The results have been compared with the existing algorithms viz. Poisson solver [21], Frankot-Chellappa algorithm[7] and diffusion using affine transformation of gradients [2]. The error behaviour in recovered depth maps and their ground truths has been reported in terms of normalized mean square error (MSE) and normalized mean absolute error (MAE) explained as follows:

- **Mean Square Error**: The ground truth height values and the evaluated height values by our proposed approach have been normalized in [0,1]. The average of the square of the difference between the normalized ground truth and evaluated normalized height values has been computed using the formula:

$$\text{MSE} = \frac{1}{MN}\sum_{y=0}^{N-1}\sum_{x=0}^{M-1}(z_1(x,y)-z_2(x,y))^2$$

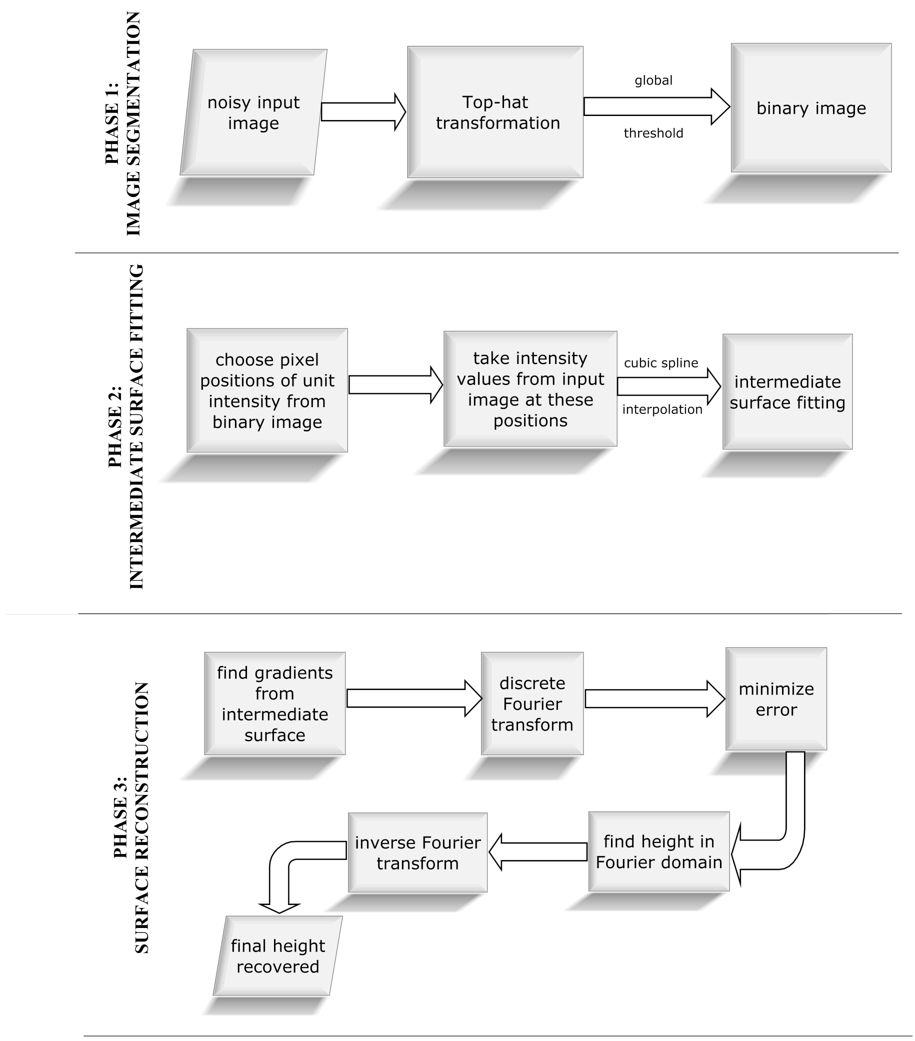

Figure 1. Block diagram for overall processs

- **Mean Absolute Error**: The ground truth height values and the evaluated height values by our proposed algorithm have been normalized in [0,1]. The mean of the absolute differences between the normalized ground truth and evaluated normalized depth values has been calculated using the formula:

$$\mathrm{MAE} = \frac{1}{MN} \sum_{y=0}^{N-1} \sum_{x=0}^{M-1} |(z_1(x,y) - z_2(x,y))|$$

where MN is the size of the image whose height is to be recovered, $z_1(x,y)$ is the ground truth height values, $z_2(x,y)$ is the evaluated height values.

The validation of our proposed algorithm has been carried out by taking standard benchmark surface of Ramp Peaks [2], ground truth surfaces of vase and Mozart. Our results have been compared with Poisson algorithm, Frankot-Chellappa algorithm and diffusion algorithm. The error analysis has been reported in Table 1.

Vase: The synthetic vase has been created by utilizing the equation given by Ascher and Carter [3] as following:

$$z(\alpha,\beta) = \sqrt{(f(\beta)^2 - \alpha^2)};$$

$$\text{where} \quad f(\beta) = 0.15 - 0.1 \times \beta \times (6\beta + 1)^2 \times (\beta - 1)^2 \times (3\beta - 2)$$

$$-0.5 \leq \alpha \leq 0.5 \quad 0 \leq \beta \leq 1$$

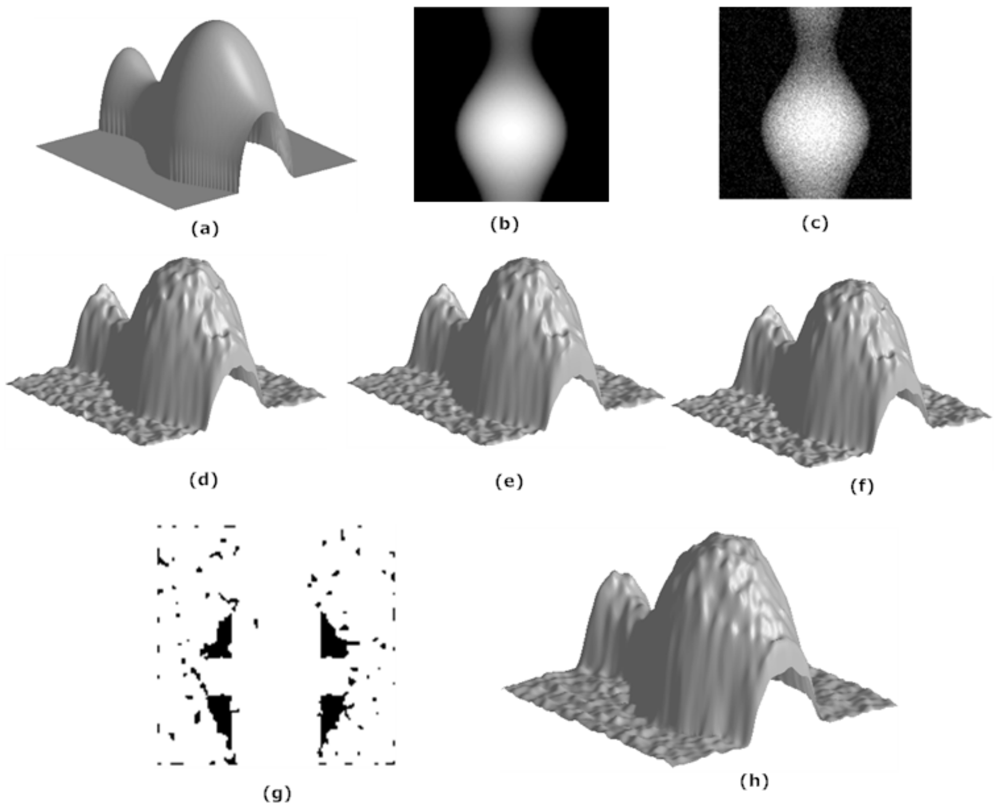

Figure 2. Reconstruction using various algorithms:(a) Ground-truth surface; (b) synthetic image; (c) noisy image; (d) reconstructed surface by Poisson solver algorithm [21]; (e) reconstructed surface by Frankot-Chellappa algorithm [7]; (f) reconstructed surface by diffusion algorithm [2]; (g) segmented image; and (h) reconstructed surface by proposed algorithm.

The ground-truth surface for this synthetic vase has been shown in Fig. 2(a). The synthetic image generated from the surface of vase is shown in Fig. 2(b). Gaussian noise has been added to the synthetic image to get a noisy image of the vase (see Fig.2(c)). Now, our aim is to reconstruct the surface of vase from this noisy 2D image. We compare our results with the algorithms viz. Poisson solver (Fig. 2(d)), Frankot-Chellapa (Fig. 2(e)) and diffusion using affine transformation of gradients (Fig. 2(f)). The obtained 3D reconstructed surface by our proposed algorithm has been shown in (Fig. 2(h)). The intermediate surface has been obtained from the segmented image figure 2(g) using cubic spline interpolation method.

Mozart: The test image has been generated from the surface data of Mozart. The ground truth depth map for Mozart has been bestowed by Professor Kuo of USC. Ground truth surface of Mozart, image generated from this surface and its corresponding noisy image have been shown in Fig. 3 (a), (b) and (c), respectively. Our algorithm has been performed very well in case of Mozart. The outcomes have been contrasted with the outcomes obtained from three different algorithms. The reconstruction of surfaces using several algorithms have been shown in Fig. 3

Ramp Peaks: The reconstructions obtained on the Ramp Peaks test surface have been shown in Fig. 4. The comparisons with other existing methods in terms of MSE and MAE have been listed in Table 1.

Real Image: Surface reconstruction has also been performed on noisy images of real data. Results have been presented in Fig. 5. It can be seen from the obtained results that the methods Poisson solver, FC algorithm and diffusion algorithm using affine transformation of gradients provide deformed and non-smooth surfaces as compared to the surface obtained with proposed method.

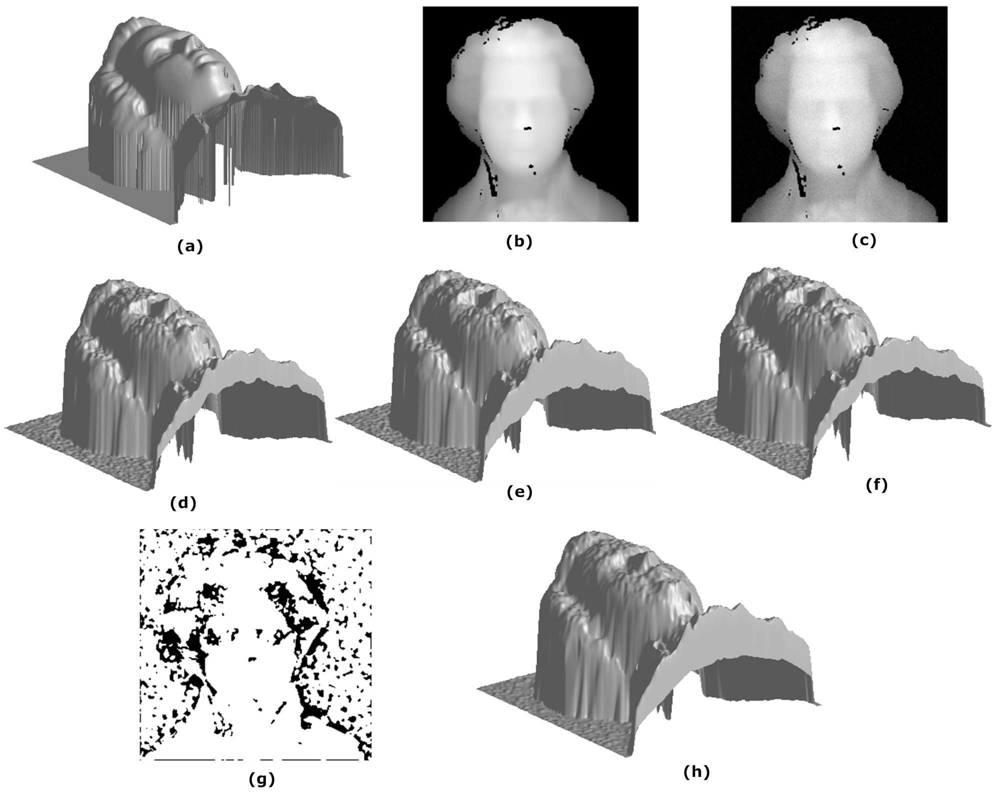

Figure 3. Reconstruction using various algorithms:(a) Ground truth surface; (b) synthetic image; (c) noisy image; (d) reconstructed surface by Poisson solver algorithm [21]; (e) reconstructed surface by Frankot-Chellappa algorithm [7]; (f) reconstructed surface by diffusion algorithm [2]; (g) segmented image; and (h) reconstructed surface by proposed algorithm.

Table 1. Normalized MSE and MAE

image	Method	MSE	MAE
Mozart	Poisson	0.1823	0.3235
	FC Algorithm	0.1856	0.3254
	Diffusion	0.1706	0.3259
	Proposed	0.0231	0.0032
Vase	Poisson	0.0956	0.2014
	FC algorithm	0.0947	0.1994
	Diffusion	0.0955	0.2048
	Proposed	0.0093	0.0649
Ramp Peaks	Poisson	0.5574	0.6580
	FC algorithm	0.6183	0.4810
	Diffusion	0.5452	0.6037
	Proposed	0.0288	0.0843

4 Conclusions

We have proposed an efficient approach to the 3D surface reconstruction from 2D image using image segmentation by mathematical morphological operations. In our approach, obtained sparse intensity data from the segmented image has been used for the generation of intermediate 3D surface using cubic spline interpolation method. The surface gradients have been calculated from the intermediate surface using central difference formulae and then final depth map has

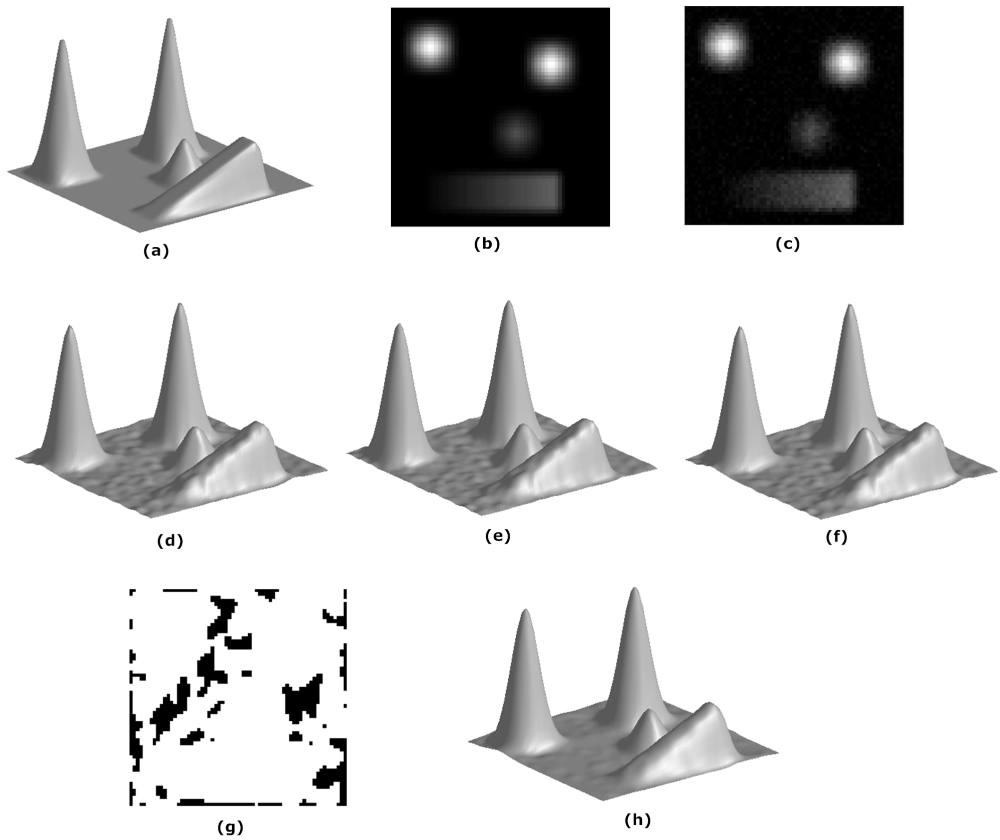

Figure 4. Reconstruction using various algorithms:(a) Ground truth surface; (b) synthetic image; (c) noisy image; (d) reconstructed surface by Poisson solver algorithm; (e) reconstructed surface by Frankot-Chellappa algorithm; (f) reconstructed surface by diffusion algorithm; (g) segmented image; and (h) reconstructed surface by proposed algorithm.

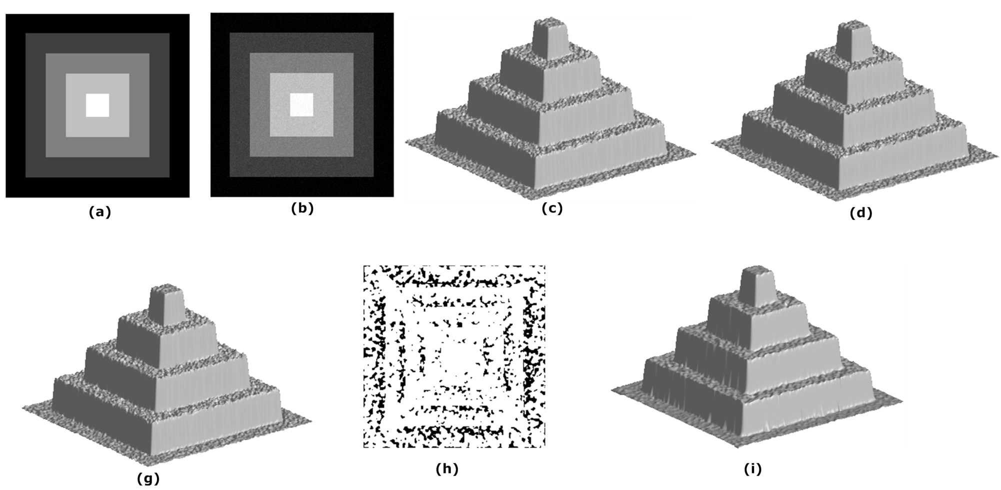

Figure 5. Reconstruction using various algorithms:(a) Real image; (b) noisy image; (c) reconstructed surface by Poisson solver algorithm; (d) reconstructed surface by Frankot-Chellappa algorithm; (e) reconstructed surface by diffusion algorithm; (f) segmented image; and (g) reconstructed surface by proposed algorithm.

been evaluated using error minimization between these gradients and the gradients of the surface to be estimated in the Fourier domain. The technique has been tested with the different set of images. Our results have been compared with the reconstructed surfaces obtained by Poisson solver, Frankot-Chellappa and diffusion algorithm using affine transformation of gradients. The results show that the proposed approach is able to acquire progressively precise depth-map as contrasted with the other algorithms. Moreover, the proposed methodology is simple to employ and gives good results in case of noisy images.

Acknowledgements

The author is grateful to the Council of Scientific & Industrial Research (CSIR), India for financial help to accomplish this research work.

References

[1] A. Agrawal, R. Chellappa, and R. Raskar. An algebraic approach to surface reconstruction from gradient fields. In *Tenth IEEE International Conference on Computer Vision(ICCV)*, volume 1, pages 174–181, 2005.

[2] A. Agrawal, R. Raskar, and R. Chellappa. What is the range of surface reconstructions from a gradient field? In *Proceedings of the 9th European Conference on Computer Vision - Volume Part I*, ECCV'06, pages 578–591, Berlin, Heidelberg, 2006. Springer-Verlag.

[3] U. M. Ascher and P. M. Carter. A multigrid method for shape from shading. *SIAM Journal on Numerical Analysis*, 30(1):102–115, 1993.

[4] H. Badri, H. Yahia, and D. Aboutajdine. Robust surface reconstruction via triple sparsity. In *IEEE Conference on Computer Vision and Pattern Recognition (CVPR) 2014*, pages 2291–2298, 2014.

[5] A. Bala, S. Kumar, R. Bhargava, and M. Agarwal. Surface reconstruction by evaluating height from gradient values. In *IEEE International Advance Computing Conference (IACC)*, pages 1033–1036, 2014.

[6] A. Bhatti, S. Nahavandi, and Y. Frayman. 3D depth estimation for visual inspection using wavelet transform modulus maxima. *Computers & Electrical Engineering*, 33(1):48 – 57, 2007.

[7] R. T. Frankot and R. Chellappa. A method for enforcing integrability in shape from shading algorithms. *IEEE Transactions on Pattern Analysis and Machine Intelligence,*, 10(4):439–451, 1988.

[8] M. Harker and P. O'Leary. Least squares surface reconstruction from gradients: Direct algebraic methods with spectral, tikhonov, and constrained regularization. In *Proceedings of the IEEE Conference on Computer Vision and Pattern Recognition*, pages 2529–2536, 2011.

[9] M. Harker and P. O'Leary. Direct regularized surface reconstruction from gradients for industrial photometric stereo. *Computers in Industry*, 64(9):1221 – 1228, 2013. Special Issue: 3D Imaging in Industry.

[10] B.K.P. Horn. Height and gradient from shading. *International Journal of Computer Vision*, 5(1):37–75, 1990.

[11] B. Karacali and W. Snyder. Noise reduction in surface reconstruction from a given gradient field. *International Journal of Computer Vision*, 60(1):25–44, 2004.

[12] P. Kovesi. Shapelets correlated with surface normals produce surfaces. In *Tenth IEEE International Conference on Computer Vision, ICCV .*, volume 2, pages 994–1001, 2005.

[13] S. Kumar, M. Kumar, B. Raman, N. Sukavanam, and R. Bhargava. Depth recovery of complex surfaces from texture-less pair of stereo images. *Electronic Letters on Computer Vision and Image Analysis*, 8(1):44–56, 2009.

[14] V. Leonardi, V. Vidal, M. Daniel, and J.-L. Mari. Multiple reconstruction and dynamic modeling of 3d digital objects using a morphing approach. *The Visual Computer*, pages 1–18, 2014.

[15] H.-S. Ng, T.-P. Wu, and C.-K. Tang. Surface-from-gradients without discrete integrability enforcement: A gaussian kernel approach. *IEEE Transactions on Pattern Analysis and Machine Intelligence*, 32(11):2085–2099, 2010.

[16] N. Otsu. A threshold selection method from gray-level histograms. *IEEE Transactions on systems, man and cybernetics.*, SMC-9(1):62–66, 1979.

[17] V. M. Patel, R. Maleh, A. C. Gilbert, and R. Chellappa. Gradient-based image recovery methods from incomplete fourier measurements. *IEEE Transactions on Image Processing,*, 21(1):94–105, 2012.

[18] D. Reddy, A. K. Agrawal, and R. Chellappa. Enforcing integrability by error correction using l1-minimization. In *IEEE Computer Society Conference on Computer Vision and Pattern Recognition (CVPR 2009)*, pages 2350–2357, 2009.

[19] R. Rosenholtz and J. Malik. Surface orientation from texture: Isotropy or homogeneity (or both)? *Vision Research*, 37(16):2283 – 2293, 1997.

[20] M. Rostami, O. Michailovich, and Z. Wang. Gradient-based surface reconstruction using compressed sensing. In *19th IEEE International Conference on Image Processing (ICIP)*, pages 913–916, 2012.

[21] T. Simchony, R. Chellappa, and M. Shao. Direct analytical methods for solving poisson equations in computer vision problems. *IEEE Transactions on Pattern Analysis and Machine Intelligence,*, 12(5):435–446, 1990.

[22] S. Someya, K. Okamoto, and G. Tanaka. 3d shape reconstruction from synthetic images captured by a rotating periscope system with a single focal direction. *Journal of Visualization*, 6(2):155–164, 2003.

[23] V. B. Surya Prasath and J. C. Moreno. On convergent finite difference schemes for variational–pde-based image processing. *Computational and Applied Mathematics*, 37(2):1562–1580, May 2018.

[24] A. Tavakoli, P. Mousavi, and F. Zarmehi. Modified algorithms for image inpainting in fourier transform domain. *Computational and Applied Mathematics*, 37(4):5239–5252, Sep 2018.

[25] T. Wei and R. Klette. Fourier transform based methods for height from gradients. In *8th Control, Automation, Robotics and Vision Conference(ICARCV)*, volume 1, pages 85–91, 2004.

[26] R. J. Woodham. Photometric method for determining surface orientation from multiple images. *Optical Engineering*, 19(1):139–144, 1980.

[27] J. Yuan, R. Gu, T. Feng, Y. Zhou, Y. Yu, and S. Du. Live three-dimensional reconstruction system with stereo vision display. *Computers & Electrical Engineering*, 39(3):818 – 833, 2013. Special issue on Image and Video Processing, Special issue on Recent Trends in Communications and Signal Processing.

[28] C. Zhu and W. Leow. Textured mesh surface reconstruction of large buildings with multi-view stereo. *The Visual Computer*, 29:609–615, 2013.

Author information

Anu Bala, Department of Mathematics, Multani Mal Modi College, Patiala-147001, Punjab, India.
E-mail: `anu@modicollege.com`